Geomorphology 153–154 (2012) 39–47

Contents lists available at SciVerse ScienceDirect

Geomorphology

journal homepage: www.elsevier.com/locate/geomorph

Inception of bed load motion beneath a bore

Nazanin Khezri, Hubert Chanson *

The University of Queensland, School of Civil Engineering, Brisbane QLD 4072, Australia

ARTICLE INFO

Article history:
Received 5 December 2011
Received in revised form 5 February 2012
Accepted 9 February 2012
Available online 17 February 2012

Keywords:
Tidal bores
Bed load motion
Inception
Longitudinal pressure gradient
Forces

ABSTRACT

A tidal bore is a series of waves propagating upstream in the river mouth as the tidal flow turns to rising in macro-tidal conditions. Some related geophysical processes include the tsunami-induced bores and uprushing bores on beaches. In the present study, the inception of sediment motion beneath tidal bores was investigated physically. No sediment motion was observed in the initially steady flow and beneath undular bores. A transient sheet flow motion was observed beneath breaking bores and the onset of sediment motion was closely linked with the passage of the roller toe. The forces acting on the movable gravel bed particles were estimated from the physical measurements. The results showed that the longitudinal pressure gradient force was the dominant contribution de-stabilising the particles and inducing the onset of sediment motion. The drag force added a sizeable contribution to maintain the upstream particle motion, although the entire sheet flow motion was brief.

1. Introduction

A tidal bore is a series of waves propagating upstream in the river mouth as the tidal flow turns to rising (Fig. 1A, B). The bore occurs during the flood tide under appropriate tidal, bathymetric and riverine conditions (Tricker, 1965; Chanson, 2011). Some related geophysical processes include the tsunami-induced bores when a tsunami wave propagating in shallow-water regions is led by a bore and the swash-induced bores on beaches when the wave runup encounters some rundown (Fig. 1C). The propagation of bores is known to play a major role in terms of sedimentary motion (Chen et al., 1990; Tessier and Terwindt, 1994; Chanson et al., 2011), although the dominant driving mechanism of sediment motion inception remains unclear.

In steady flows, a number of studies used photographic and video techniques to investigate the bed load motion (Sumer and Oguz, 1978; Nino and Garcia, 1998). Despite a few studies in gradually varied flows (Bombar et al., 2011), no systematic study was performed in highly unsteady open channel flows. In such rapidly-varied flows, the large scale vortices may play an important role in terms of sediment pickup and, when the turbulent mixing length is much larger than the sediment distribution length scale, the validity of the Shields diagram application is arguable (Nielsen, 1992). The present study examines the propagation of tidal bores with a focus on the mechanisms of sediment transport inception. The analysis is based upon a physical study based upon a Froude dynamic similarity performed on a movable gravel bed. The results based upon individual particle motion show the relative significance of longitudinal pressure gradient and drag forces beneath the bore. It is the aim of this work to characterise the seminal features of bed load motion inception beneath tidal bores and to provide quantitative details such as particle velocities and accelerations to improve future sediment transport models.

1.1. Theoretical considerations

In unsteady open channel flow phenomena such as a bore propagating over movable beds (Fig. 2), the forces acting on each sediment particle include the gravity force, the buoyancy force, the shear/drag force, the lift force, the resultant of the reaction forces of the surrounding grains (or intergranular force), the longitudinal pressure gradient, the Magnus force, the virtual mass force and the Basset history force. The buoyancy and gravity forces act along the vertical, the drag force along the flow direction and the lift force in the direction perpendicular to the flow (Fig. 2). For a submerged sediment particle on the horizontal channel bed, Newton's law of motion applied to the particle in the longitudinal direction yields in first approximation:

$$m_s \frac{\partial V_s}{\partial t} = F_{drag} + F_p + F_{virtual} + \left(F_{grain}\right)_x + F_{Basset} \quad (1)$$

where m_s is the particle mass, V_s is the horizontal particle velocity component and the forces acting on the particle initially at rest are the drag force F_{drag}, a longitudinal pressure gradient force F_p, a virtual mass force $F_{virtual}$, the intergranular force component in the horizontal direction $(F_{grain})_x$ and the Basset history force. Since this study is concerned with the onset of sediment motion,

* Corresponding author. Tel.: +61 7 3365 4163; fax: +61 7 3365 4599.
E-mail address: h.chanson@uq.edu.au (H. Chanson).

0169-555X/$ – see front matter © 2012 Elsevier B.V. All rights reserved.
doi:10.1016/j.geomorph.2012.02.006

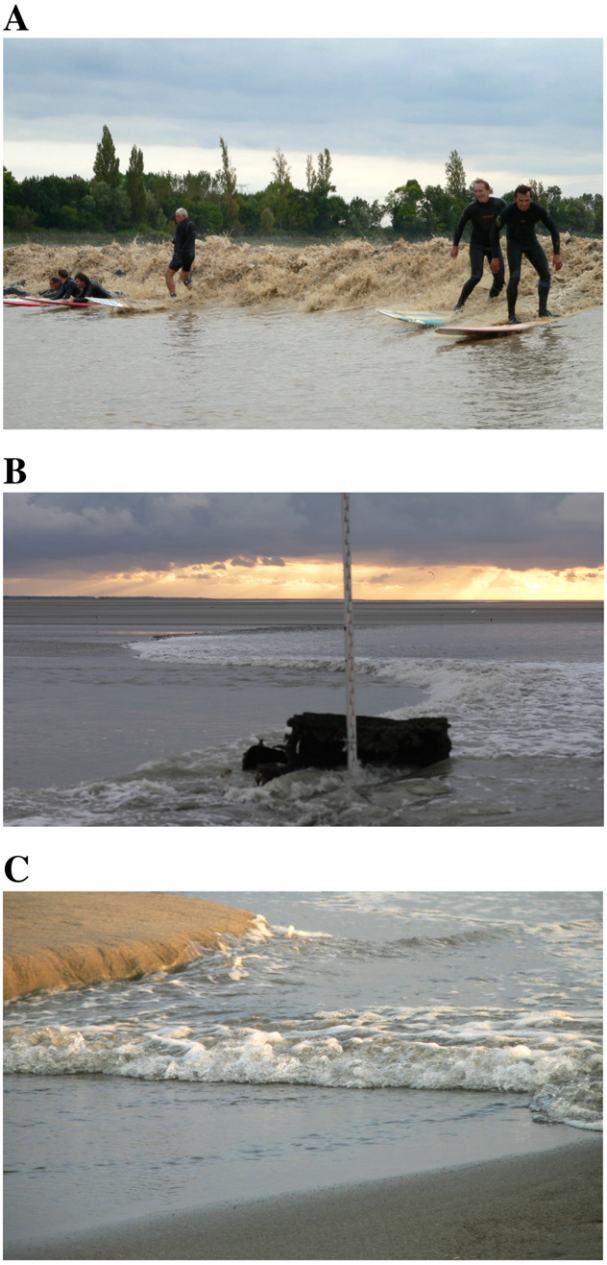

Fig. 1. Photographs of bores — bore propagation from right to left. (A) Tidal bore of the Dordogne River at Asques (France) on 30 September 2008 afternoon, U~2 m/s. (B) Tidal bore of the Sélune River at Vains (France) on 24 September 2010, d_o = 0.38 m, U = 2.0 m/s, Fr = 2.35. (C) Swash-induced bore in a small inlet at Ikobe Beach, Enshu coast (Japan) on 14 November 2008, d_o~0.05 m, U~0.5 m/s.

the particle is initially at rest and the Basset history term will be assumed small in the following paragraphs, while the intergranular force is commonly unknown.

For a particle in motion, the drag force is:

$$F_{drag} = \frac{1}{2} C_d \rho (V_x - V_s)|V_x - V_s| A_s \quad (2)$$

where C_d is the drag coefficient, ρ is the water density, V_x is the longitudinal water velocity component positive downstream, $|V_x|$ is the velocity component magnitude, A_s is the projected area of the sediment particle, and the particle velocity V_s is positive downstream.

In presence of a longitudinal pressure gradient $\partial P/\partial x$ as beneath a tidal bore (Fig. 2), the longitudinal pressure force on a fixed particle is:

$$F_p = -\frac{\partial P}{\partial x} A_s h_s \quad (3a)$$

where P is the pressure, h_s is a characteristic particle dimension and x is the longitudinal direction positive downstream (Fig. 2). For a spherical particle with diameter d_s, the longitudinal pressure gradient force equals:

$$F_p = -\frac{\partial P}{\partial x} \frac{\pi}{6} d_s^3 \quad (3b)$$

In Eq. (3), the longitudinal pressure gradient $\partial P/\partial x$ is assumed constant across the particle, an assumption which might not be accurate for large particles beneath to the roller toe.

The virtual mass force is:

$$F_{virtual} = \frac{m_s}{s} C_m \frac{\partial (V - V_s)}{\partial t} \quad (4)$$

where s is the particle relative density and C_m is an added mass coefficient function of the particle shape and flow conditions (Brennen, 1982).

2. Experimental apparatus and methods

2.1. Experimental facility

The inception of sediment motion beneath a bore was investigated physically in a relatively large flume at the University of Queensland (Figs. 3 and 4). The test section was 12 m long and 0.5 m wide with a PVC bed and glass side walls. The waters were supplied by a constant head reservoir feeding into a large intake, 2.1 m long, 1.1 m wide and 1.1 m deep, leading to the test section through a smooth convergent. At the channel downstream end (x = 11.15 m), where x is the distance from the channel upstream end, a fast-closing tainter gate was installed.

The water discharge was measured with two orifice meters designed based upon the British Standards (British Standard, 1943) and calibrated on site with a volume per time method. The percentage of error was estimated to be less than 2%. In steady flows, the water depths were measured using rail mounted pointer gauges. The unsteady water depths were recorded with a series of acoustic displacement meters. A Microsonic™ Mic + 35/IU/TC unit was located at x = 10.8 m, where x is the longitudinal distance from the test section upstream end. Three acoustic displacement meters Microsonic™ Mic + 25/IU/TC were installed above the channel at x = 4, 5 and 6 m. The acoustic displacement meters were calibrated against the pointer gauges in steady flows.

The velocity measurements were performed using an acoustic Doppler velocimeter Nortek™ Vectrino + (Serial No. VNO 0436) equipped with a three-dimensional side-looking head (Fig. 3). The velocity range was 1.0 m/s and the sampling rate was 200 Hz. The data accuracy was 1% of the velocity range. Both the acoustic displacement meters and acoustic Doppler velocimeter were synchronised within +/−1 ms. The translation of the ADV probe in the vertical direction was controlled by a fine adjustment travelling mechanism connected to a Mitutoyo™ digimatic scale unit, with an error on the vertical position of less than 0.025 mm. The accuracy on the longitudinal position was estimated as $\Delta x < \pm 2$ mm. All the measurements were taken on the channel centreline. The post-processing of the ADV signal was limited to a removal of communication errors, although the vertical velocity component V_z data might be affected adversely by the bed proximity for z < 0.030 m.